Novel dynamic model of self-excited induction generator with iron losses

Mateo Bašić, Dinko Vukadinović and Duško Lukač

***Abstract*—** In this paper, we propose a novel dynamic model of a self-excited induction generator (SEIG), in which the iron losses are included and represented as a variable parameter, dependent on both air-gap flux and stator frequency. The air-gap flux influence is expressed by means of the corresponding iron loss current. In addition, the iron losses are modeled by means of a variable equivalent iron loss resistance, connected in parallel with the magnetizing reactance. To determine the iron loss resistance as well as the magnetizing inductance of the actual induction machine, we performed a series of no-load tests over a wide range of frequencies, using sinusoidal supply. In order to provide this kind of supply for the induction machine, we used a synchronous generator driven by a DC motor. In addition, we built the proposed dynamic model of a SEIG in the MATLAB/Simulink environment. This is, to the best knowledge of the authors, the first SEIG model with variable iron losses that was entirely built in Simulink. In order to analyze the performance of the proposed model, we carried out a number of simulations and experiments. It is shown that the proposed model better approximates the actual induction machine in comparison with the conventional model, in which the iron losses are neglected.

Keywords— Dynamic model, Efficiency, Iron losses, Self-excited induction generator.

I. Introduction

In general, a self-excited induction generator (SEIG) is an induction generator with capacitor excitation. Although self-excitation process has been known since the 1930s [1], [2], until recently it was not possible to effectively utilize it. Nowadays, SEIGs are particularly preferred in stand-alone applications, of power up to 100 kW, that employ wind or hydro power [3]. In such applications they offer several advantages compared with the conventional synchronous generators, as can be found in [4]. On the other hand, SEIGs are characterized by poor voltage and frequency regulation, and by low power factor.

Self-excitation of an induction generator occurs only when a suitable capacitance is connected across the stator terminals. For a particular capacitance value, it is possible to define a corresponding minimum rotor speed needed for initiation of the self-excitation process and vice versa [1], [5]. The generated voltage builds up through the process of self-excitation until it finally settles at a certain value, which is, for given speed and capacitance, mainly determined by the magnetizing inductance saturation. Once the SEIG is loaded, both frequency and magnitude of the generated voltage change because of a non-zero slip value, even when the rotor speed is kept constant.

This paper focuses on the effect the iron losses have on the SEIG's performance at various operating conditions. In conventional SEIG models, for the sake of convenience, the iron losses are usually entirely neglected. However, even in the machines with low amount of iron losses, their impact is not negligibly small. Moreover, neglecting the iron losses of an induction machine is reported to cause detuning within a corresponding vector control system [6]. In literature, even when the iron losses are considered within an induction machine model, they are usually presented as constant [7] or linearly dependent on the air-gap voltage [8], [9]. However, in the actual machine, the iron losses vary with both air-gap flux and stator frequency. Hence, in order to get a more accurate prediction of the induction machine's performance, it is necessary to consider these influences. This is especially important when modeling a SEIG because of the variable flux levels and speeds (i.e. frequencies) they work with. In addition, since accurate assessment of SEIG behavior during transients is not possible using steady state models [10]-[12], a dynamic model of a SEIG is needed.

In this paper, we propose and analyze a novel dynamic model of a SEIG in which the iron losses are represented as a function of both air-gap flux and stator frequency. The proposed model is compared with the conventional SEIG model in which the iron losses are entirely neglected. Given that the iron losses are always present in induction machines, it is expected that the proposed SEIG model better approximates the actual induction machine in comparison with the conventional SEIG model. Since this paper is focused exclusively on the analysis of the induction generator model, turbine is not specifically modeled. Instead, the rotor speed is taken as an independent and variable input into the model.

II. SEIG Model with Variable Iron Losses

The iron losses are usually represented in the induction machine model with an equivalent iron loss resistance R_m connected in parallel or in series with the magnetizing reactance X_m, where the power loss of the equivalent resistance is equal to the total iron losses in the induction machine. Fig. 1 actually presents the conventional stationary reference frame (α-β) model of an induction machine with the equivalent iron loss resistance added across the magnetizing branch.

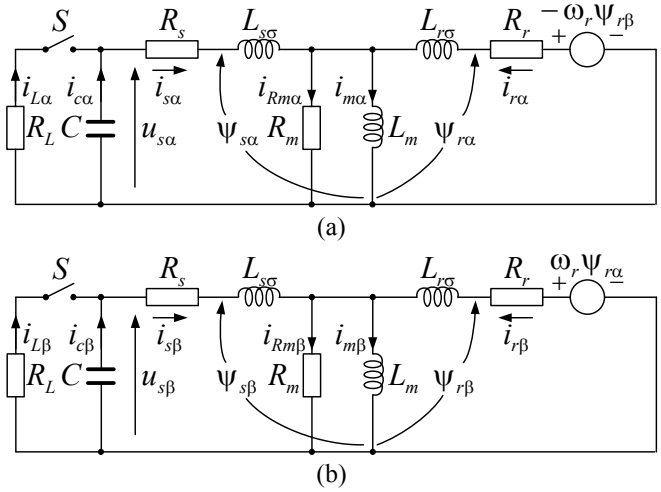

Fig. 1 Stationary reference frame model of SEIG with equivalent iron loss resistance R_m: (a) α-axis, (b) β-axis

In addition, a parallel combination of an excitation capacitor and a resistive load is connected at the stator terminals. The load is connected across the capacitor through the switch *S*. The SEIG is, however, always started at no load and it is loaded only when the steady state is reached.

The mathematical model of an induction machine, obtained from Fig. 1, is presented by the following set of equations in the stationary α-β reference frame:

$$u_{s\alpha} = R_s i_{s\alpha} + \frac{d\psi_{s\alpha}}{dt}$$

$$u_{s\beta} = R_s i_{s\beta} + \frac{d\psi_{s\beta}}{dt} \tag{1}$$

$$0 = R_r i_{r\alpha} + \frac{d\psi_{r\alpha}}{dt} + \omega_r \psi_{r\beta}$$

$$0 = R_r i_{r\beta} + \frac{d\psi_{r\beta}}{dt} - \omega_r \psi_{r\alpha} \tag{2}$$

$$\psi_{s\alpha} = L_{s\sigma} i_{s\alpha} + L_m i_{m\alpha}$$

$$\psi_{s\beta} = L_{s\sigma} i_{s\beta} + L_m i_{m\beta} \tag{3}$$

$$\psi_{r\alpha} = L_{r\sigma} i_{r\alpha} + L_m i_{m\alpha} + \psi_{r\beta o}$$

$$\psi_{r\beta} = L_{r\sigma} i_{r\beta} + L_m i_{m\beta} + \psi_{r\alpha o} \tag{4}$$

$$R_m i_{Rm\alpha} = L_m \frac{di_{m\alpha}}{dt}$$

$$R_m i_{Rm\beta} = L_m \frac{di_{m\beta}}{dt} \tag{5}$$

$$i_{m\alpha} + i_{Rm\alpha} = i_{s\alpha} + i_{r\alpha}$$

$$i_{m\beta} + i_{Rm\beta} = i_{s\beta} + i_{r\beta} \tag{6}$$

$$T_e = \frac{3}{2} p \frac{L_m}{L_r} \left[\psi_{r\alpha} \left(i_{s\beta} - i_{Rm\beta} \right) - \psi_{r\beta} \left(i_{s\alpha} - i_{Rm\alpha} \right) \right] \tag{7}$$

where:

$u_{s\alpha}$, $u_{s\beta}$, $i_{s\alpha}$, $i_{s\beta}$, $\psi_{s\alpha}$ and $\psi_{s\beta}$ are α and β components of the stator voltage space-vector, the stator current space-vector and the stator flux linkage space-vector, respectively;

$i_{r\alpha}$, $i_{r\beta}$, $\psi_{r\alpha}$ and $\psi_{r\beta}$ are α and β components of the rotor current space-vector and the rotor flux linkage space- vector, respectively;

$i_{Rm\alpha}$, $i_{Rm\beta}$, $i_{m\alpha}$ and $i_{m\beta}$ are α and β components of the iron loss current space-vector and the magnetizing current space-vector, respectively;

R_s, R_r and R_m are the stator resistance, the rotor resistance and the iron loss resistance, respectively;

$L_{s\sigma}$, $L_{r\sigma}$ and L_m are the stator leakage inductance, the rotor leakage inductance and the magnetizing inductance, respectively;

ω_r is the rotor angular speed expressed in electrical radians per second;

T_e is the induced electromagnetic torque and p is the number of the pole pairs.

In (4), $\psi_{r\alpha o}$ and $\psi_{r\beta o}$ represent the residual rotor flux linkages along the α and β axis, respectively.

The capacitor and load voltages are equal to the stator voltages and can be expressed as follows:

$$u_{c\alpha} = u_{s\alpha} = \frac{1}{C} \int_0^t i_{c\alpha} dt + u_{s\alpha o}$$

$$u_{c\beta} = u_{s\beta} = \frac{1}{C} \int_0^t i_{c\beta} dt + u_{s\beta o} \tag{8}$$

$$u_{L\alpha} = u_{s\alpha} = R_L i_{L\alpha}$$

$$u_{L\beta} = u_{s\beta} = R_L i_{L\beta} \tag{9}$$

where $u_{s\alpha o}$ and $u_{s\beta o}$ are the initial voltages along the α and β axis capacitors, respectively, C is the excitation capacitance and R_L is the resistive load.

Furthermore, the stator currents can be expressed as the sum of the respective load and capacitor currents as follows:

$$i_{s\alpha} = i_{L\alpha} + i_{c\alpha}$$

$$i_{s\beta} = i_{L\beta} + i_{c\beta} . \tag{10}$$

By comparison with the conventional model, the only additional datum required in realization of the proposed model is the value of the equivalent iron loss resistance, which could be easily obtained during the commissioning procedure.

A. Determination of the iron loss resistance characteristics

As previously mentioned, if an induction generator is operating at variable flux levels and speeds, the iron loss resistance R_m should be represented as a function of both stator frequency and air-gap flux. Since iron losses have to be identified experimentally, we performed a series of standard no-load tests over a wide range of frequencies. Fig. 2 shows the no-load test experimental setup.

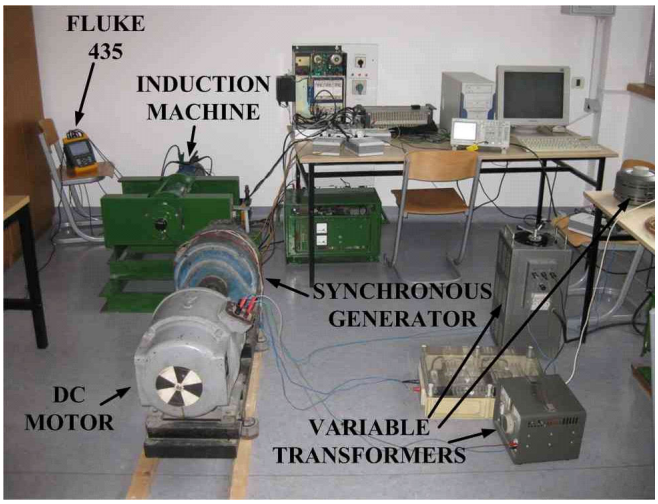

Fig. 2 No load tests experimental setup

In order to provide sinusoidal supply at the induction machine terminals, we used a synchronous generator driven by a DC motor. The measured data were obtained by means of both Fluke 435 power quality analyzer and conventional analog instruments. Frequencies encompassed within performed tests were from 10 Hz to 60 Hz.

In general, the iron losses found from no-load testing may be used for assessing performance during loading when an induction machine is driven up to rated load. We used the procedure described in [13] to identify the equivalent iron loss resistance and magnetizing reactance from the measured data. Once when the iron loss resistance is identified in the frequency range of interest, it becomes possible to express it as both stator frequency and magnetizing flux dependent parameter. In this paper, the air-gap flux influence is expressed by means of the corresponding iron loss current, i_{Rm}. Obtained characteristics of the iron loss resistance versus no-load iron loss current, I_{Rmo}, with the operating frequency as parameter, are presented in Fig. 3.

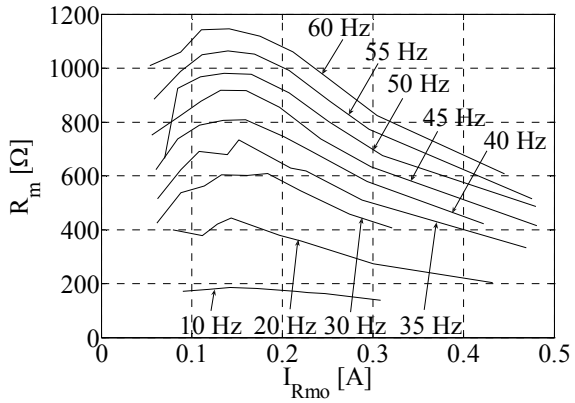

Fig. 3 Measured equivalent iron loss resistance characteristics

It is evident from Fig. 3 that the iron loss resistance value significantly depends on both stator frequency and iron loss current.

B. Determination of the magnetizing inductance characteristic

For SEIGs, the magnetizing inductance saturation is the main factor for buildup and stabilization of the generated voltage. Hence, inclusion of the magnetizing inductance, L_m, variation with the magnetizing current, I_m, within a SEIG model is a must. We determined this variation experimentally, within the same set of no-load tests described in the previous chapter. Fig. 4 presents measured magnetizing inductance characteristics, obtained at seven various frequencies in the range from 30 Hz to 60 Hz. The discrepancy between the characteristics is so small that it can barely be seen with the given scale. Hence, it can be concluded that the magnetizing inductance is frequency independent.

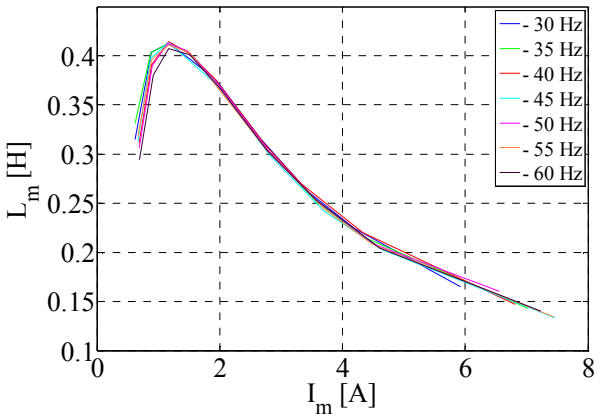

Fig. 4 Measured magnetizing inductance characteristics

Consequently, final magnetizing inductance characteristic is obtained by approximation of the measured characteristics. In [14], the functions defined in [15] and [16] were used for the magnetizing inductance approximation. However, it turned out that the accuracy of the approximation, especially in the saturation area, is of crucial importance to the overall accuracy of the model. For the operating regime given in Chapter III *B*, e.g., the approximation error of ±5 % increases/decreases the generated voltage magnitude for about ±8.5 %. Therefore, in this paper, we paid a special attention to the accurate approximation of the measured characteristics. Consequently, final magnetizing inductance characteristic is obtained from the measured values by using the interpolation-extrapolation method (look-up table). Constant unsaturated value of the magnetizing inductance (L_m^n) is set as equal to 0.4058 H (for the magnetizing currents lower than 1.437 A). However, since SEIG's equilibrium point is always located somewhere in the saturated part of the characteristic (I_m > 1.437 A), this part of the characteristic is critical.

C. Proposed Simulink Model of a Self-Excited Induction Generator

From (1) - (6) and using Laplace transformation, four 2nd order differential equations are obtained as follows:

$$s^2 i_{s\alpha} = -\left(\frac{R_s}{L_{\sigma s}} + \frac{R_m}{L_m} + \frac{R_m}{L_{\sigma s}}\right) s i_{s\alpha} - \frac{R_s R_m}{L_{\sigma s} L_m} i_{s\alpha} - \frac{R_m}{L_{\sigma s}} s i_{r\alpha} - \frac{1}{L_{\sigma s}} s u_{s\alpha} - \frac{R_m}{L_{\sigma s} L_m} u_{s\alpha} \quad (11)$$

$$s^2 i_{s\beta} = -\left(\frac{R_s}{L_{\sigma s}} + \frac{R_m}{L_m} + \frac{R_m}{L_{\sigma s}}\right) s i_{s\beta} - \frac{R_s R_m}{L_{\sigma s} L_m} i_{s\beta} - \frac{R_m}{L_{\sigma s}} s i_{r\beta} - \frac{1}{L_{\sigma s}} s u_{s\beta} - \frac{R_m}{L_{\sigma s} L_m} u_{s\beta} \quad (12)$$

$$s^2 i_{r\alpha} = -\frac{R_m}{L_{\sigma r}} s i_{s\alpha} - \left(\frac{R_r}{L_{\sigma s}} + \frac{R_m}{L_m} + \frac{R_m}{L_{\sigma r}}\right) s i_{r\alpha} - \omega_r s i_{r\beta} - \omega_r \frac{R_m}{L_{\sigma r}} i_{s\beta} - \frac{R_r R_m}{L_{\sigma r} L_m} i_{r\alpha} - \omega_r R_m \left(\frac{1}{L_{\sigma r}} + \frac{1}{L_m}\right) i_{r\beta} - \frac{1}{L_{\sigma r}} s K_{r\alpha} - \frac{R_m}{L_{\sigma r} L_m} K_{r\alpha} \quad (13)$$

$$s^2 i_{r\beta} = -\frac{R_m}{L_{\sigma r}} s i_{s\beta} - \left(\frac{R_r}{L_{\sigma s}} + \frac{R_m}{L_m} + \frac{R_m}{L_{\sigma r}}\right) s i_{r\beta} + \omega_r s i_{r\alpha} + \omega_r \frac{R_m}{L_{\sigma r}} i_{s\alpha} - \frac{R_r R_m}{L_{\sigma r} L_m} i_{r\beta} + \omega_r R_m \left(\frac{1}{L_{\sigma r}} + \frac{1}{L_m}\right) i_{r\alpha} + \frac{1}{L_{\sigma r}} s K_{r\beta} + \frac{R_m}{L_{\sigma r} L_m} K_{r\beta} \quad (14)$$

where $K_{r\alpha}$ and $K_{r\beta}$ are constants, which represent the initial induced voltages due to residual magnetizing flux in the iron core along the α and β axis, respectively. Similar set of equations is given in [8], but it contains several algebraic sign errors which have been corrected.

Using (11) - (14) we built a simulation model of a SEIG in MATLAB/Simulink environment. This is, to the best knowledge of the authors, the first SEIG model including variable iron losses that is entirely built in Simulink. The model is presented in Figs. 5 and 6. The inputs to the "SEIG-Rm" block, which represents the induction generator, are ω_r, $K_{r\alpha}$, $K_{r\beta}$, $u_{s\alpha o}$, $u_{s\beta o}$, C and R_L, whereas the outputs are $u_{s\alpha}$, $u_{s\beta}$, $i_{s\alpha}$, $i_{s\beta}$, $i_{r\alpha}$, $i_{r\beta}$ and T_e. The initial voltages along the α and β axis, the rotor speed and the capacitance are all presented by means of constant value blocks, whereas loading of the generator is implemented by means of a step function block. The stator angular frequency ω_e is obtained by derivation of the stator voltage space-vector angle. Gray colored local subsystem blocks in Fig. 6 represent (7), (11) - (14) and the magnetizing inductance estimation algorithm.

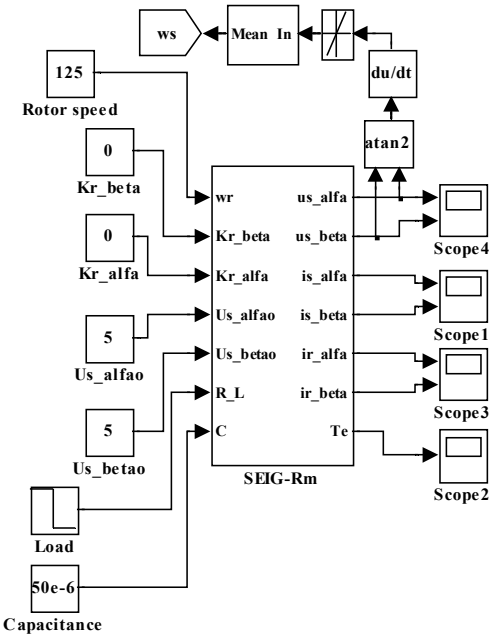

Fig. 5 Proposed SEIG model in Simulink

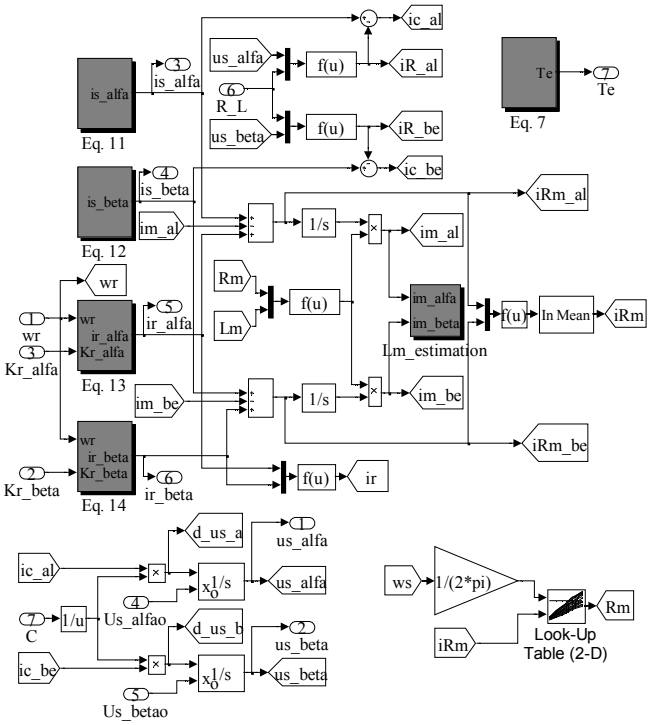

Fig.6 "SEIG-Rm" subsystem block

The equivalent iron loss resistance is obtained as the look-up table output with the stator frequency and the iron loss current used as the inputs. The initial value of the iron loss resistance was set to 800 Ω (for I_{Rm} < 0.07 A).

III. Performance Analysis of the Enhanced SEIG Model

In order to evaluate the validity of the proposed SEIG modeling approach, performance of the proposed simulation

model is analyzed under various operating conditions and compared with the conventional SEIG model, in which the iron losses are entirely neglected. In addition, the proposed model is verified experimentally. Parameters of the induction machine used in this investigation are given in Appendix.

The approximate minimum capacitance value required for self-excitation to occur under no load conditions can be calculated as follows, [8]

$$C_{\min} \approx \frac{1}{\omega_r^2 L_m^n}. \tag{15}$$

However, it is not advisable to use the minimum capacitance value because any change in load or rotor speed values may result in loss of excitation. On the other hand, it is also not advisable to choose excessive capacitance values due to economic and technical reasons. In this paper, about 25 % overestimated capacitance values were used.

A. Simulation Results

We carried out the simulations of the following two operating regimes:

1. The rotor speed was fixed at 125 rad/s. At $t = 3$ s, the SEIG was loaded with the resistive load of 220 Ω. The capacitance value was fixed at 50 μF.
2. The rotor speed was fixed at 140 rad/s. At $t = 3$ s, the SEIG was loaded with the resistive load of 150 Ω. The capacitance value was fixed at 40 μF.

In both simulations, initial voltages along the α and β axis are fixed at 5 V, while initial voltages due to remanence are neglected and, hence, fixed at 0 V.

The results obtained from running the first simulation are shown in Figs. 7 to 11. Fig. 7 shows that the inclusion of the iron losses within the model extended the magnetization process (about 0.15 s longer) and reduced the generated voltage magnitude. The maximum steady state difference between the two stator voltage space vector magnitudes occurred while the SEIG was loaded and is equal to 2.07 %. Moreover, the stator voltage space vector magnitudes were notably decreased due to loading (about 10 %). The maximum obtained steady state difference between the two stator current space vector magnitudes is equal to 2.54 % (Fig. 8). As it can be seen from Fig. 9, inclusion of the iron losses increased the rotor current space-vector magnitude. However, since the rotor current is considerably smaller than the stator current, it has a considerably smaller impact on the overall losses. In addition, the SEIG's efficiency is calculated as the ratio between the electrical output power and the shaft input power. The calculated efficiencies are equal to 83.77 % and 67.25 %, for the conventional model and for the proposed model, respectively. This large efficiency deterioration of 16.52 % is due to iron losses only.

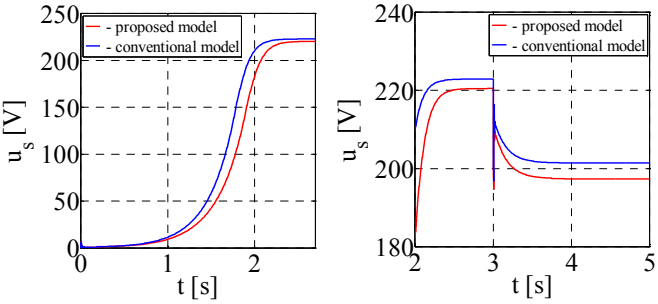

Fig. 7 Stator voltage space vector module: (a) magnetization, (b) loading

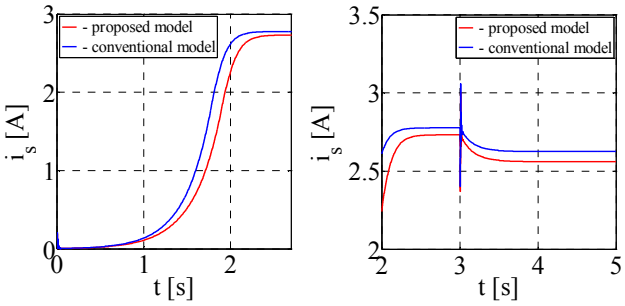

Fig. 8 Stator current space vector module: (a) magnetization, (b) loading

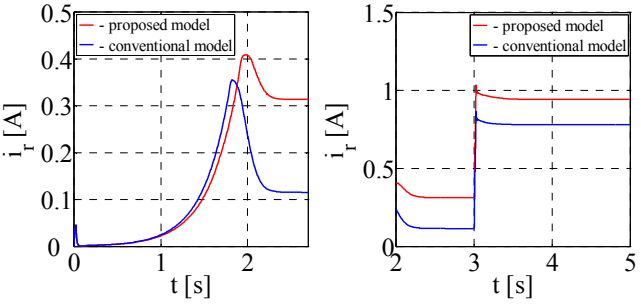

Fig. 9 Rotor current space vector module: (a) magnetization, (b) loading

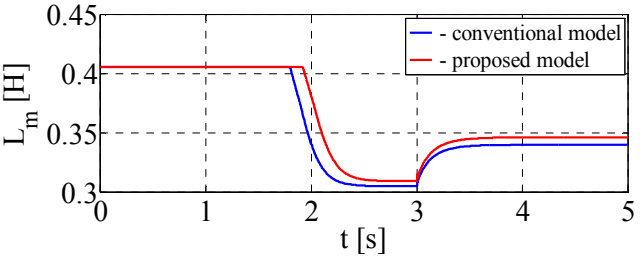

Fig. 10 Magnetizing inductance

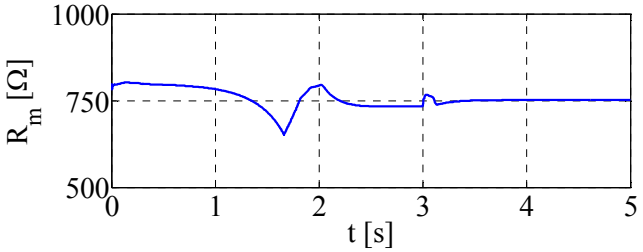

Fig. 11 Equivalent iron loss resistance

The results obtained from running the second simulation are shown in Figs. 12 to 16. Similar conclusions can be drawn as in the first simulation. In this case, the magnetization process was extended for about 0.13 s due to iron losses. The maximum obtained steady state difference between the two stator voltage space vector magnitudes is equal to 3.02 % (Fig. 12). Due to loading, the stator voltage space-vector magnitudes decreased for about 22 %. This higher voltage magnitude drop, compared with the first simulation, is due to implementation of more excessive load. The maximum obtained steady state difference between the two stator current space vector magnitudes is equal to 3.36 % (Fig 13). Finally, the efficiency deterioration of 11.09 % is noted. In this case, the efficiency deterioration is smaller than in the first simulation. This is due to higher value of the equivalent iron loss resistance and, therefore, lower iron losses.

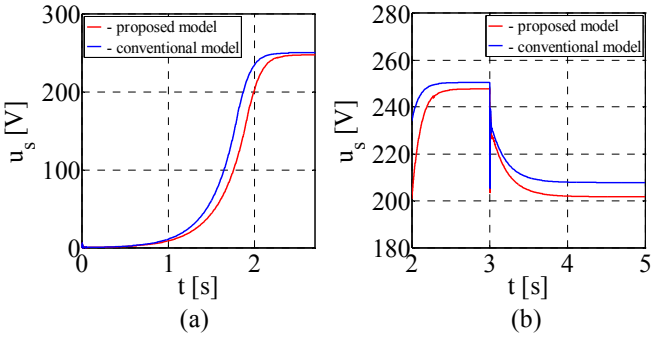

Fig. 12 Stator voltage space vector module:
(a) magnetization, (b) loading

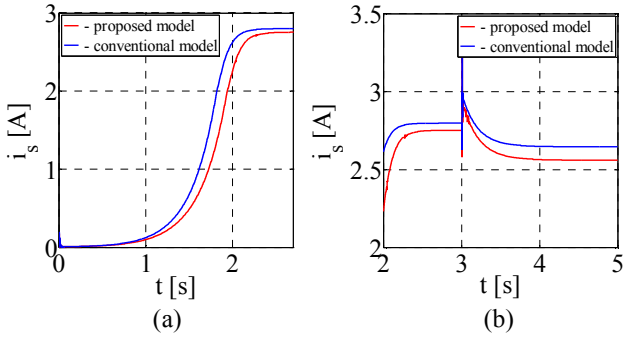

Fig. 13 Stator current space vector module:
(a) magnetization, (b) loading

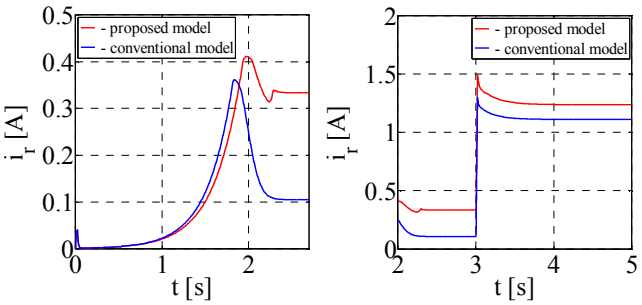

Fig. 14 Rotor current space vector module:
(a) magnetization, (b) loading

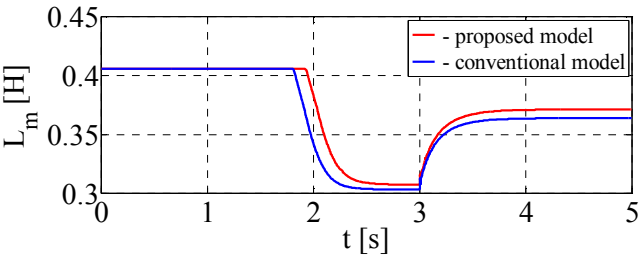

Fig. 15 Magnetizing inductance

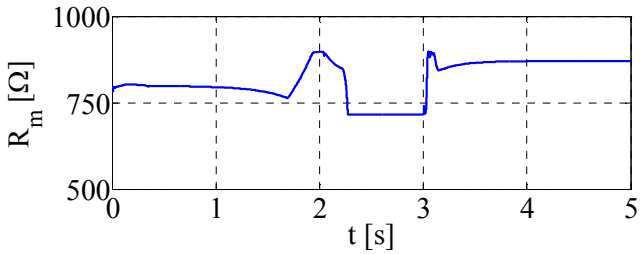

Fig. 16 Equivalent iron loss resistance

In general, when the iron losses are neglected, generated voltage and electrical output power of a SEIG are higher than for the case when the iron losses are included. On the other hand, neglecting the iron losses results in lower mechanical input power and, therefore, the higher overall efficiency of a SEIG is obtained. In addition, the highest differences between the generated voltage/current magnitudes obtained from the two induction generator models used in this investigation are within 5 %, which can be interpreted as negligible.

B. Experimental Results

The SEIG experimental setup is presented in Fig. 17. We used a DC motor with a speed controller as the induction generator prime mover. DC motor speed was controlled by means of SIMOREG DC-MASTER converter, type 6RA7031, manufactured by Siemens [17]. In addition, all of the measured quantities were collected by means of the digital signal processing (dSpace DS1104 microcontroller board).

We carried out the following experiment: the rotor speed was held constant at 1200 r/min (≈ 125 rad/s) and at $t = 4$ s, the SEIG was loaded with the resistive load R_L = 220 Ω. We used the fixed capacitance value of 50 μF.

Fig. 17 SEIG experimental setup

In addition, the above mentioned operating regime was also simulated by using both conventional and proposed model. To achieve a better comparison of the experimental results with the results obtained from the simulations, we recreated and employed the measured speed signal within the simulations by means of a signal builder block.

Experimentally obtained results, along with the simulation results, are shown in Figs. 18 to 23. As it can be seen from Fig. 18, connecting the load at the stator terminals resulted in 3.71 % speed transient drop. On Figs. 19 and 20 there is a certain difference noticeable between the measured and simulated voltages and currents due to additional losses in the actual machine. However, the difference is evidently smaller within the proposed model. The maximum steady state difference between the measured RMS value of the stator phase voltage and the one obtained from the proposed model occurred while the SEIG was loaded and it is equal to 1.42 %. The maximum steady state difference between the measured RMS value of the stator phase current and the one obtained from the proposed model also occurred while the SEIG was loaded and has a percentage value of 0.55 %. Moreover, the RMS values of the stator phase voltage were decreased due to loading by 11.33 % - obtained from the measurement and by 10.53 % - obtained from the proposed model. Speed transient drop caused the generated voltage undershoot (4.33 % - measured voltage undershoot, 2.54 % - proposed model voltage undershoot and 2.72 % - conventional model voltage undershoot). From Fig. 21, it can be concluded that the proposed model very well estimates the actual output power. Namely, for the considered operating regime, the steady state difference between the measured output power and the one obtained from the proposed model is equal to 3.29 W (1.21 %), whereas the difference between the measured output power and the one obtained from the conventional model is equal to 7.65 W (2.8 %). At the same time, the steady state difference between the measured input power and the one obtained from the proposed model is equal to 35.56 W (8.15 %), whereas the difference between the measured input power and the one obtained from the conventional model is equal to 101.6 W (23.28 %). The efficiency values are equal to 62.46 % - measured, 67.18 % - obtained from the proposed model and 83.69 % - obtained from the conventional model.

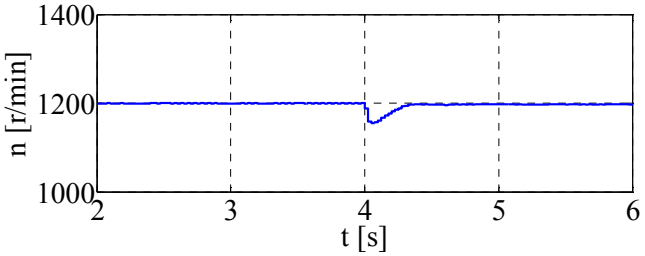

Fig. 18 Measured rotor speed

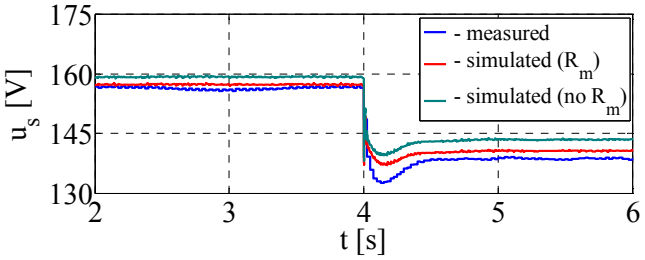

Fig. 19 RMS value of stator phase voltage

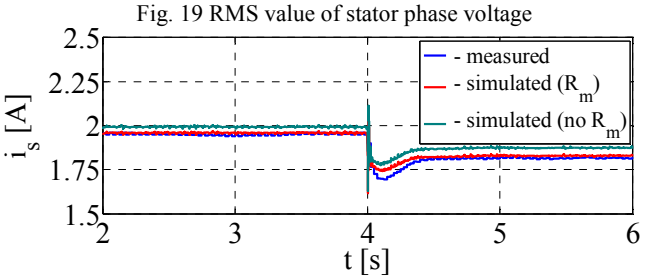

Fig. 20 RMS value of stator phase current

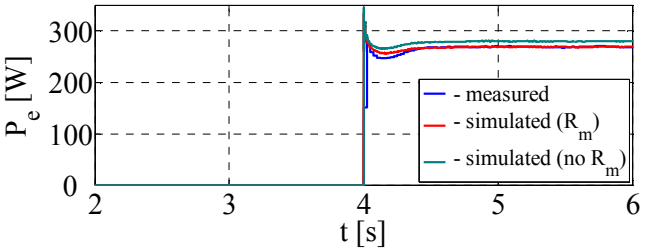

Fig. 21 Electrical output power

Moreover, in order to determine how the rotor speed variation affects the overall efficiency and input power, additional measurements were carried out. Fig. 22 presents the efficiency variation with the rotor speed, for two various capacitance values. The results were obtained for the resistive load of 220 Ω.

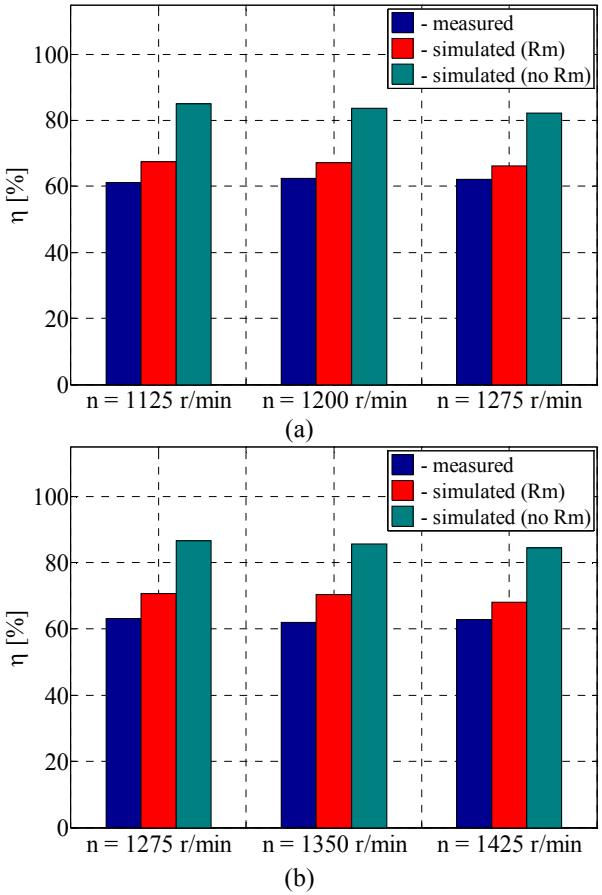

Fig. 22 Efficiency variation with speed (R_L = 220 Ω):
(a) C = 50 μF, (b) C = 40 μF

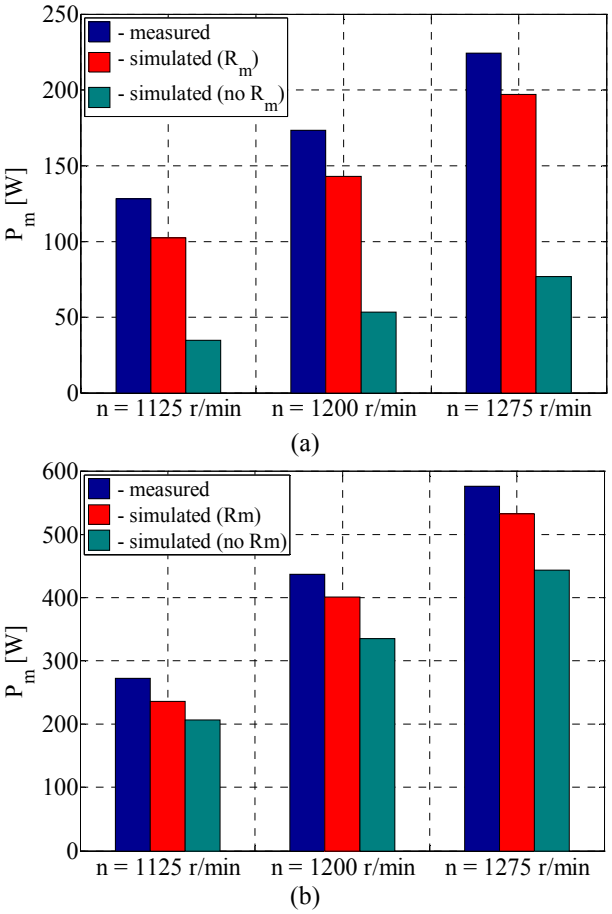

Fig. 23 Mechanical input power variation with speed (C = 50 μF):
(a) no-load, (b) R_L = 220 Ω

For the considered speed range, the efficiency values obtained from the proposed model are obviously much closer to the measured efficiency values, compared with the efficiency values obtained from the conventional model. The maximum difference between the efficiency value obtained from the proposed model and the one obtained from the measurements, for the same speed, is equal to 8.04 % (4.07 % - minimum), whereas the maximum difference between the efficiency obtained from the conventional model and the measured one is equal to 23.75 % (20.16 % - minimum). These large efficiency estimation errors that occur within the conventional model are mainly due to inaccurately estimated input power. When the proposed SEIG model is used, these inaccuracies are significantly reduced, as it can be seen in Fig 23. Inaccuracy of the input power obtained from the conventional SEIG model is especially emphasized at no-load conditions. This is because at no-load conditions the iron losses have a more dominant part in the overall SEIG losses than when a SEIG is loaded. Therefore, neglecting the iron losses when a SEIG is not loaded has a more significant impact on the accuracy of the input power estimation.

IV. Conclusion

From simulation and experimental results, several important conclusions are drawn:

- When analyzing the overall efficiency and/or input power demand of a SEIG, inclusion of the iron losses into the SEIG model is mandatory.
- In order to represent the iron losses more accurately, they should be expressed as a function of both air-gap flux and stator frequency, especially when they vary considerably.
- If only generated voltages and currents are considered within the SEIG's performance analysis, the conventional SEIG model presents a good enough approximation of the actual machine.
- The conventional SEIG model gives a fairly good estimation of the actual output power but, at the same time, introduces a significant error in estimating the input power, which results in poor estimation of the overall efficiency.
- The error in estimating the magnetizing inductance less than 5 % can significantly deteriorate the performance of the model, regardless of which model is used.
- The proposed model gives better estimation of measured generated voltages and currents, and significantly better estimation of the measured efficiency, in comparison with

the conventional model.

- A close agreement of simulation and experimental results proves the validity of the proposed model.

APPENDIX

P_n=1.5 kW, U_n=380 V, p=2, Y, I_n=3.81 A, n_n=1391 r/min, L_m^n =0.4058 H, $L_{\sigma s}$=0.01823 H, $L_{\sigma r}$=0.02185 H, R_s=4.293 Ω, R_r=3.866 Ω (at 20 °C), T_n=10.5 Nm, J=0.0071 kgm^2.

REFERENCES

[1] C. Wagner, "Self-excitation of Induction Motors", *Trans. AIEE*, vol.58, pp. 47–51, February 1939.

[2] E. D. Basset, F. M. Potter, "Capacitive Excitation for Induction Generators", *Trans. AIEE,* vol.54, no.5, pp. 540–545, May 1935.

[3] T. F. Chan, "Analysis of Self-Excited Induction Generators Using an Iterative Method", *IEEE Transactions on Energy Conversion*, vol.10, no.3, pp. 502-507, September 1995.

[4] G. K. Singh, "Self-Excited Induction Generator Research - A Survey", *Electric Power Systems Research*, vol.69, no.2-3, pp. 107-114, May 2004.

[5] C. Grantham, D. Sutanto, and B. Mismail, "Steady-state and Transient Analysis of Self-Excited Induction Generators", in *Proc. Inst. Elect. Eng., pt. B,* 1989, pp. 61–68.

[6] E. Levi, M. Sokola, A. Boglietti, M. Pastorelli, "Iron Loss in Rotor-flux-oriented Induction Machines: Identification, Assessment of Detuning, and Compensation", *IEEE Transactions on Power Electronics*, vol.11, no.5, pp. 698-709, September 1996.

[7] R. Leidhold, G. Garcia, and M. I. Valla, "Field-Oriented Controlled Induction Generator With Loss Minimization", *IEEE Transactions on Industrial Electronics*, vol.49, no.1, pp. 147-156, February 2002.

[8] D. Seyoum, "The Dynamic Analysis and Control of a Self-Excited Induction Generator Driven by a Wind Turbine", Ph. D. thesis, School of Electrical Engineering and Telecommunications, UNSW, Sydney, Australia, 2003.

[9] S. D. Wee, M. H. Shin, and D. S. Hyun, "Stator-Flux-Oriented Control of Induction Motor Considering Iron Loss", *IEEE Transactions on Industrial Electronics*, vol.48, no.3, pp. 147-156, June 2001.

[10] K. S. Sandhu and D. Joshi, "Steady State Analysis of Self-Excited Induction Generator using Phasor-Diagram Based Iterative Model" *WSEAS Transactions on Power Systems*, vol. 3, no. 12, pp. 715-724, December 2008.

[11] K. S. Sandhu and D. Joshi, "A Simple Approach to Estimate the Steady-State Performance of Self-Excited Induction Generator" *WSEAS Transactions on Systems and Control*, vol. 3, no. 3, pp. 208-218, March 2008.

[12] K. S. Sandhu, "Steady State Modeling of Isolated Induction Generators" *WSEAS Transactions on Environment and Development*, vol. 4, no. 1, pp. 66-77, January 2008.

[13] I. Boldea and S. A. Nasar, *The Induction Machine Handbook*, CRC Press, 2002.

[14] M. Bašić, D. Vukadinović, and D. Lukač, "Analysis of an Enhanced SEIG Model Including Iron Losses", in *Proc. 6th WSEAS Int. Conf. EEESD and 3rd WSEAS Int. Conf. LA*, Timisoara, 2010, pp. 37-43.

[15] D. Vukadinović and M. Smajo, "Analysis of Magnetic Saturation in Induction Motor Drives", *International Review of Electrical Engineering*, vol.3, no.2, pp. 326-336, April 2008.

[16] D. Vukadinović, M. Smajo, and Lj. Kulišić, "Rotor Resistance Identification in an IRFO System of a Saturated Induction Motor", *International Journal of Robotics and Automation*, vol.24, no.1, pp. 38-47, 2009.

[17] *Simoreg DC-Master Operating Instructions*, Siemens, Edition 13, 2007, Available: http://www.sea.siemens.com/us/Products/Drives/DC-Drives/Pages/DC-Master-Manuals.aspx

Mateo Bašić was born in Split, Croatia, in 1982. He received the B.E. degree from the University of Split, Croatia, in 2006, in electrical engineering. He became an assistant at the University of Split, Faculty of Electrical Engineering, Mechanical Engineering and Naval Architecture, Department of Electric Power Engineering, in 2008. He is pursuing the Ph.D. degree in electrical engineering at the University of Split, Split, Croatia.

He has co-authored a number of papers published in scientific journals and conference proceedings. His current research interests include self-excited induction generators, induction machine control systems and power electronics.

Dinko Vukadinović was born in Banja Luka, Bosnia and Herzegovina, in 1973. He received the B.E. degree from the University of Split, the M.E. degree from the University of Zagreb and the Ph.D. degree from the University of Split, Croatia, in 1997, 2002 and 2005, respectively, all in electrical engineering. He became a junior researcher in the University of Split, Faculty of Electrical Engineering, Mechanical Engineering and Naval Architecture, Department of Electric Power Engineering, in 1998. In 2006, he became an Assistant Professor at the University of Split. He is an Associate Editor of the Journal of Engineering, Computing & Architecture and Journal of Computer Science, Informatics and Electrical Engineering.

He has published a number of papers in major scientific journals. His research interests include induction machine control systems, power electronics, digital signal processors and artificial intelligence.

Dr. Vukadinović is a member of the KES International.